

Exact analysis of long distance quantum communication over a lossy optical channel using entanglement swapping with a quantum repeater chain and noisy detectors

Zachary Dutton, Christopher A. Fuchs, Saikat Guha, and Hari Krovi
*Quantum Information Processing group, Raytheon BBN Technologies,
 10 Moulton Street, Cambridge, MA 02138, USA*

We analyze a long-distance entanglement based quantum key distribution (QKD) architecture, which uses multiple linear-optic quantum repeaters, frequency-multiplexed entanglement sources, and classical error correction. We find an exact expression for the secret-key rate, and an analytical characterization of how errors propagate through noisy repeater links, as a function of all loss and noise parameters, when the sources have zero multi-pair emissions, i.e., $g^2(0) = 0$. We also present numerical results that show that two-pair-emission rates of a downconversion source has an unworkably poor rate-distance scaling, and show how the performance improves as $g^2(0)$ of the source decreases. Our analysis of how the entangled state held by the two distant parties evolves through multiple swap operations, can in principle be applied to other repeater architectures as well. The exact results and scaling laws we present, may provide new quantitative insights useful not only for designing long-distance QKD architectures, but for all distributed quantum information protocols that require establishing long-distance entanglement.

Shared entanglement underlies many quantum information protocols such as quantum key distribution [1], teleportation [2] and superdense coding [3], and is a fundamental information resource that can boost both classical and quantum communication over noisy quantum channels [4, 5]. Optical photons are arguably the best candidates for distributing entanglement across long distances, albeit they are extremely susceptible to loss and noise in the channel, which is the bane of practical realizations of long-distance quantum communication. The maximum entanglement-generation rate over a lossy optical channel with no classical-communication assistance goes to zero for loss exceeding 3 dB. With classical communication assistance, entanglement generation capacity decays linearly with the channel's transmittance (i.e., exponentially with optical fiber length) for loss exceeding ~ 5 dB [6]. Thus in order to generate entanglement over long distances at high rates, quantum repeaters must be used, interspersed along the lossy channel.

Several quantum repeater protocols have been proposed, which use entanglement swapping by Bell state measurements, and quantum memories of some form (See [7] for a recent review). The basic quantum repeater is a scheme that overcomes the exponential decay of entanglement-distribution rate with the length of the channel, by connecting a string of imperfect entangled pairs of particles by using a nested purification protocol, thereby creating a single distant pair of high fidelity [8]. An alternative (the DLCZ) repeater protocol uses a chain of elementary links between pairs of atomic memories created in single-photon entangled states, followed by a distant heralded interferometric conversion of two copies of such entangled state into a two-photon entangled state. These protocols rely on purifying multiple long-distance imperfect shared entangled pairs (into one pair of high fidelity). As an alternative to entanglement purification, a coded-repeater architecture was proposed that generates

a backbone of encoded Bell pairs and uses classical error correction during simultaneous entanglement connections [10], whose performance—in terms of its classical communication overhead—was found to surpass that of the standard architecture [11]. In [12], a repeater architecture was proposed that uses quantum memories based on atomic ensembles and linear optics for Bell state measurements [13, 14]. This protocol does not rely on entanglement purification, does not require one to hierarchically connect the elementary links (i.e., multiple connections can proceed simultaneously), lets the fidelity (of the shared entangled state) propagate through the chain, and use classical error correction at the reconciliation stage to extract shared secret keys. One of the biggest challenges that faces practical designs of long-distance quantum repeater architectures, is the quantitative understanding of how the shared entangled state evolves across concatenated swap operations across multiple quantum repeater nodes. Some recent studies were done to analyze quantum repeater chains [12, 15, 16], which either used extensive numerical simulations, or proposed semi-analytic or approximate theoretical models.

In this paper, we present a complete analytic characterization of the evolution of the shared-entangled state in a concatenated quantum repeater chain, as proposed in [12], which uses single-photon entangled states and linear-optic Bell-state analyzers comprised of lossy and noisy single-photon detectors. Our analysis technique can in principle be applied to other repeater architectures as well. We obtain an exact expression for the secret key rate as a function of distance, number of swap stages, and loss-and-noise parameters of the channel and detectors. We find a compact scaling law for how the quantum bit error rate (QBER)—the probability that Alice and Bob obtain a mismatched raw bit despite measuring their halves of the entangled state in the same bases—scales with increasing number of swap

levels. This analytical scaling has important practical importance, since a measured QBER on a single elementary link can be used to predict the QBER (and hence the key rates) in a long-distance link, constructed with imperfect devices. This calculation involves a detailed analysis of the swap operations by modeling imperfect single-photon detectors with appropriate positive-operator-valued-measure (POVM) elements, and solving a variant of the *logistic map*, whose solutions are chaotic in general [17]. Since we calculate the exact quantum state after every swap stage, our results can be used to calculate any other quantity of interest, such as fidelity, in other applications of long-distance shared entanglement. We also simulate the repeater chain numerically, to confirm our theory. Our efficient simulation, which uses sparsified matrix representations of bosonic operations, enable us to go beyond sources with $g^2(0) = 0$. A non-zero two-pair probability $p(2)$ is shown to rapidly deteriorate the rate-distance scaling. The $g^2(0)$ of spontaneous parametric downconversion (SPDC) sources render them essentially useless for long-distance QKD, even with repeater chains. As $g^2(0) \approx 2p(2)/p(1)^2$ is lowered toward zero, the secret key rate is shown to scale progressively better. Even for sources with $g^2(0) > 0$, our analytic prediction of error propagation through repeater chains is shown to hold, albeit with a $p(2)$ -dependent modification to a pre-factor.

The paper is organized as follows. We begin with a description of the repeater architecture. We then state our main results, followed by a high-level description of the key steps of our theoretical analysis. Detailed proofs are deferred to the Supplementary Material. Finally, we summarize our main numerical results, followed by a description of our results on the effect of source imperfections on the scaling of the secret key rate, in detail. We conclude with thoughts on open questions and future work.

THE QUANTUM REPEATER ARCHITECTURE

The architecture [12] is depicted schematically in Figs. 1, 2. The total range (distance from Alice to Bob) is L km of lossy fiber, divided into $N = 2^n$ elementary links.

The elementary links.—At the center of each elementary link, a linear-optic Bell-state measurement (BSM) [13] acts on the halves of two pairs of maximally-entangled Bell states, $|M^\pm\rangle \triangleq [|10, 01\rangle \pm |01, 10\rangle]/\sqrt{2}$, each sent through a lossy channel of transmissivity $\lambda = 10^{-(\alpha L/2N)/10}$, where α (in dB/km) is the fiber's loss coefficient. The BSM at the center of each elementary link comprises a 50-50 beam-splitter followed by a pair of spectrally-resolved single-photon detector arrays to detect across M frequencies. The detection efficiencies and dark-click probability per mode for each detector is taken

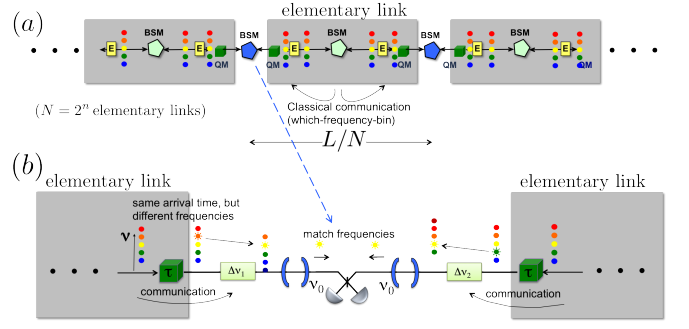


Figure 1. Schematic of quantum repeater architecture [12].

to be η_e and P_e , respectively. A linear-optic BSM is successful with at most 50% probability [14]. Each qubit, encoded in two temporal modes (of each frequency mode), occupies T_q seconds. The entangled photon-pair sources E at each end of the elementary link are assumed to be deterministic sources that generate a copy of $|M^\pm\rangle$ each, every T_q seconds. Each source sends two modes (of the 4) towards the BSM at the center of the elementary link over a lossy channel. The remaining two modes are loaded to a broadband atomic quantum memory [18]. Treating a perfect $|M^\pm\rangle$ state suffices since all the channel loss (and zero-photon emission probability at the source) can be *pushed* through the beam-splitter of the BSM device into a multiplier to the detection efficiency η_e of the detectors. Upon successful projection by the BSM on one of the two Bell states (the linear-optic BSM never projects on two of the four Bell states)—in at least one of the M frequencies, which happens with probability $P_s(1) = 1 - (1 - P_{s0})^M$, the BSM communicates the which-frequency information to both memories. P_{s0} is the probability of successful creation of an elementary link for a single frequency mode. We denote the quantum state of a successfully-created elementary link, as ρ_1 .

Connecting elementary links.—Each quantum memory receives a pair of which-frequency information from two elementary links (see Fig. 1(b)), which it uses to translate the qubits from the two sides to a pre-determined common frequency [12], and thereafter performs a linear-optic BSM. Let us denote the detection efficiencies and dark-click probability per mode for each of the two detectors used for the BSM, η_r and P_r , respectively. Let λ_m denote a sub-unity transmittance to account for inefficiency in loading the qubit into the memory. If this BSM is successful, two elementary links are connected to form an entangled state across twice the distance of ρ_1 . We denote the state of this connected segment, ρ_2 . Two copies of ρ_2 are connected (probabilistically) to produce ρ_3 , and so on. Given two identical copies of ρ_{i-1} , we denote the probability that one copy of ρ_i is created, $P_s(i)$, for $1 \leq i \leq n + 1$.

Error probabilities and key rate.—Let us assume that Alice and Bob both make a measurement on each qubit

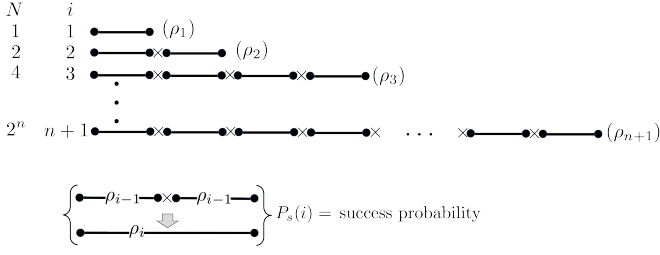


Figure 2. Concatenated linking of $N = 2^n$ elementary links.

of the entangled state ρ_i at their respective ends, either in the computational basis (single-photon detection on each of the two modes), or the 45% rotated basis (realized by a 50-50 beamsplitter between the two modes of the qubit, followed by single-photon detection on each mode). Let us denote the detection efficiency and dark-click probability per mode for their detectors, η_d and P_d , respectively. Let P_1 be the probability that they *both* obtain exactly one click (on the two modes of the measured qubit) when they measure in matching bases. Conditioned on this event happening, we denote Q_i to be the probability the raw bits Alice and Bob infer are different (despite the fact they deemed the measurement successful). The error correcting code used to extract shared secure keys must code around this error rate. Clearly, if all detectors in the architecture are noiseless (i.e., $P_e = P_r = P_d = 0$), $Q_i = 0$, $1 \leq i \leq n+1$. The overall success probability in creating ρ_{n+1} , $P_{\text{succ}} = P_s(n+1) P_s(n)^2 \dots P_s(2)^{2^{n-1}} P_s(1)^{2^n}$. If Alice and Bob work with ρ_{n+1} , i.e., have $N = 2^n$ elementary links separating them, the unconditionally-secure secret key rate they can extract is given by,

$$R = \frac{P_1 P_{\text{succ}} R_2(Q_{n+1})}{2T_q} \text{ secret-key bits/sec}, \quad (1)$$

where the factor of 2 in the denominator accounts for the probability that Alice and Bob use the same basis choice, $R_2(Q) = 1 + 2(1-Q)\log_2(1-Q) + 2Q\log_2(Q)$ is the secret-key rate of BB84 in bits per sifted symbol, with Q the error probability in the sifted raw bit [19, 20].

THEORETICAL ANALYSIS

Main results.—The main theoretical results are to derive explicit formulas for P_{succ} , P_1 , and Q_{n+1} , and hence a completely analytical characterization of the secret key rate (1). The results are summarized below.

Theorem 1 *Assuming Alice and Bob make a measurement on ρ_i in the same basis,*

1. Sift probability. *The probability they both get exactly one click each (and hence deem their measurement outcomes useful) is given by, $P_1 = (q_1 + q_2)^2$, where $q_1 = (1 - P_d)A_d$ and $q_2 = (1 - A_d)P_d$, with*

$A_d \equiv \eta_d + (1 - \eta_d)P_d$, are loss and noise parameters of Alice's and Bob's detectors.

2. QBER. *Conditioned on a successful sift, the error probability Q_i , i.e., the probability they obtain mismatched bits, is given by,*

$$Q_i = \frac{1}{2} \left[1 - \frac{t_d}{t_r} (t_r t_e)^{2^{i-1}} \right], \quad 1 \leq i \leq n+1, \quad (2)$$

where $t_e = (1 - 2w_1)/(1 + 2w_1)$, $t_r = (1 - 2w_r)/(1 + 2w_r)$, and $t_d = ((q_1 - q_2)/(q_1 + q_2))^2$ are functions of loss-noise parameters of detectors in the elementary links, memory (repeater) nodes, and Alice-Bob, respectively, which become one when the respective detector has zero dark-click probability. $2w_1 = 2c_e/(a_e + b_e)$, is the relative probability of classical correlations to that of pure Bell states in the elementary link state ρ_1 . $2w_r = 2c/(a + b)$ is the fractional probability spillovers to the classical states at each repeater connection. (See Proposition 2 for remaining definitions.)

3. Successful connection probabilities. *The success probability $P_s(i)$, to prepare ρ_i from two copies of ρ_{i-1} , is given by, $P_s(1) = s_1 = a_e + b_e + 2c_e$, and $P_s(i) = s = a + b + 2c$, for $2 \leq i \leq n+1$. The overall success probability is therefore given by,*

$$P_{\text{succ}} = \frac{1}{4s} [4s(1 - (1 - 4s_1)^M)]^{2^n}. \quad (3)$$

The proof of Theorem 1 involves a detailed analysis of how the quantum states ρ_i evolve through successive connections of elementary links (sketched in Fig. 2) and finding the exact solution of a variation of the so called *logistic map* (whose solutions are chaotic in general). With the Q_i as defined above, it is easy to see that,

$$(1 - 2Q_{i+1}) = \frac{t_r}{t_d} (1 - 2Q_i)^2, \quad 1 \leq i \leq n. \quad (4)$$

The pre-factor t_r/t_d in the above error-propagation law equals one if the detectors at the memory nodes have zero dark clicks ($P_r = 0 \Rightarrow t_r = 1$) and if the detectors used to measure the end points of ρ_i have zero dark clicks ($P_d = 0 \Rightarrow t_d = 1$). One interesting observation about the error propagation (4) is that the constant t_r is only a function of the fractional probability transferred to classical correlations (2c) to that which goes to one of two Bell states ($a + b$), when two pure Bell states are connected by a linear-optic BSM with lossy-noisy detectors (see Proposition 2).

Proof sketch of Theorem 1.—We now describe the steps leading up to the proof of the results summarized in Theorem 1. We will defer several details to the Supplementary Material. We first explicitly calculate the quantum state ρ_i after a given number of elementary links are successfully connected, and thereafter use that to calculate

Q_i , P_1 , P_{succ} , and eventually the end-to-end secret-key rates using Eq. (1). Note that we can assume without loss of generality that the sources always produce the single-photon state $|M^+\rangle$. In reality, the sources may produce $|M^+\rangle$ or $|M^-\rangle$ probabilistically, and the signs can be accounted for in post processing at the error-correction stage. Let us first consider calculating the states, ρ_i .

Proposition 2 *The quantum state ρ_i obtained after i connection levels, $1 \leq i \leq n+1$, is given by,*

$$\rho_i = \frac{1}{s_i} [a_i |M^+\rangle \langle M^+| + b_i |M^-\rangle \langle M^-| + c_i |\psi_0\rangle \langle \psi_0| + d_i |\psi_1\rangle \langle \psi_1| + d_i |\psi_2\rangle \langle \psi_2| + c_i |\psi_3\rangle \langle \psi_3|], \quad (5)$$

where $|\psi_0\rangle = |01, 01\rangle$, $|\psi_1\rangle = |01, 10\rangle$, $|\psi_2\rangle = |10, 01\rangle$, $|\psi_3\rangle = |10, 10\rangle$, $|M^\pm\rangle = [|\psi_2\rangle \pm |\psi_1\rangle]/\sqrt{2}$, $s_i = a_i + b_i + 2(c_i + d_i)$ is a normalization constant, and the coefficients of ρ_{i+1} are recursively given as:

$$a_{i+1} = \frac{1}{s_i^2} [aa_i^2 + (a+b)a_i b_i + bb_i^2], \quad (6)$$

$$b_{i+1} = \frac{1}{s_i^2} [ba_i^2 + (a+b)a_i b_i + ab_i^2], \quad (7)$$

$$c_{i+1} = \frac{1}{s_i^2} [c(a_i + b_i)^2 + 2(a+b)c_i(a_i + b_i + 2d_i) + 4c(d_i(a_i + b_i) + c_i^2 + d_i^2)], \quad (8)$$

$$d_{i+1} = \frac{1}{s_i^2} [4cc_i(a_i + b_i + 2d_i) + 2(a+b)(d_i(a_i + b_i) + c_i^2 + d_i^2)], \text{ with} \quad (9)$$

$$s_{i+1} = a_{i+1} + b_{i+1} + 2(c_{i+1} + d_{i+1}), \quad (10)$$

where the parameters,

$$a = \frac{1}{8} [P_r^2(1 - A_r)^2 + A_r^2(1 - P_r)^2], \quad (11)$$

$$b = \frac{1}{8} [2A_r P_r(1 - A_r)(1 - P_r)], \quad (12)$$

$$c = \frac{1}{8} P_r(1 - P_r) [P_r(1 - B_r) + B_r(1 - P_r)], \quad (13)$$

with $A_r = \eta_r \lambda_m + P_r(1 - \eta_r \lambda_m)$, and $B_r = 1 - (1 - P_r)(1 - \eta_r \lambda_m)^2$, are functions of the system's loss and noise parameters. For $i = 1$ (the elementary link), we have the initial conditions, $a_1 = a_e$, $b_1 = b_e$, $c_1 = c_e$, and $d_1 = 0$, with $s_1 = a_e + b_e + 2c_e$, where a_e, b_e, c_e are defined exactly as a, b, c , with (P_e, A_e, B_e) replacing (P_r, A_r, B_r) in Eqs. (6), (7), (8), where $A_e = \eta_e \lambda + P_e(1 - \eta_e \lambda)$ and $B_e = 1 - (1 - P_e)(1 - \eta_e \lambda)^2$, defined similar to A_r, B_r .

This proposition is proved in the Supplementary Material, where we also calculate the state ρ_i (i.e., the coefficients a_i, b_i, c_i, d_i) explicitly for all i in terms of the loss and noise parameters. The key steps in the proof are: (i) to realize that the transmittance of half of each elementary link λ and the memory efficiency λ_m at the repeater nodes, can be combined with the

detector efficiencies η_e and η_r of the BSs, respectively, (ii) realizing that a single-photon detector with efficiency η and dark-click probability P —when the light impinging on it is guaranteed to have no more than 2 photons—is accurately described by the POVM elements, $F_0 = (1-P)\Pi_0 + (1-P)(1-\eta)\Pi_1 + (1-P)(1-\eta)^2\Pi_2$ and $F_1 = \mathbb{I} - F_0$, with $\Pi_i = |i\rangle\langle i|$, $i = 0, 1, 2$ are projectors corresponding to the vacuum, single photon and two photon outcomes of an ideal photon-number-resolving measurement, and, (iii) carrying out the BSM on $\rho_i^{\otimes 2}$ while accounting for the appropriate post-selections [14].

Once we have the state ρ_i , defined recursively in terms of ρ_{i-1} , we calculate the success probabilities, $P_s(i) = 4s_i$. The key is to realize that $s_i = s = a + b + 2c$, $\forall i \geq 2$, which follows from adding Eqs. (6) and (7). The success probability of creating ρ_1 , $P_s(1) = 1 - (1 - P_{s0})^M$, where $P_{s0} = 4s_1$ is the probability of successful creation of an elementary link ρ_1 in one of the M frequencies.

We next prove that the sift-probability $P_1 = (q_1 + q_2)^2$, $\forall i$, where $q_1 = (1 - P_d)A_d$, $q_2 = (1 - A_d)P_d$, with $A_d = \eta_d P_d + 1 - \eta_d$ are parameters of Alice's and Bob's noisy detectors. An intuitive explanation is as follows: q_2 is the probability that the noisy detector 'flips' the outcome ($|10\rangle$ detected as (no-click, click), or $|01\rangle$ detected as (click, no-click)), whereas q_1 is the probability that the detector does not flip the outcome ($|01\rangle$ detected as (no-click, click), or $|10\rangle$ detected as (click, no-click)). Since the flip and no-flip probabilities are symmetric in the inputs $|01\rangle$ and $|10\rangle$, and each half of ρ_i has exactly one photon, regardless of the relative fraction of $|01\rangle$ and $|10\rangle$ in Alice's and Bob's states, the probability they both get a single-click outcome is $(q_1 + q_2)^2$.

The final step is to obtain the error probability $Q_i = \text{Tr}[\rho_i(M_{0101} + M_{1010})]/\text{Tr}[\rho_i(M_{0101} + M_{0110} + M_{1001} + M_{1010})]$ (note that the denominator is P_1), with $M_{ijkl} \equiv F_i \otimes F_j \otimes F_k \otimes F_l$. It is simple to argue that Q_i is a function only of $2c_i/s_i$ (see Supplementary Material for detailed proof). The intuitive argument is that a bit error only arises from $2c_i/s_i$, the fractional probability of the classical correlation terms in ρ_i , whereas $(a_i + b_i)$ is the sum fractional probability of the two Bell states $|M^+\rangle$ (a_i) and $|M^-\rangle$ (b_i), with $s_i = (a_i + b_i) + 2c_i$. Even if the BSM results accidentally in a $|M^-\rangle$ to be formed, there would be no bit error. In order to calculate c_i , we calculate $c_i + d_i \equiv y_i$ and $c_i - d_i \equiv u_i$ by adding and subtracting Eqs. (8) and (9), and writing recursions for y_i and u_i . The solution to y_i comes out as, $y_i = (s_i - z_i)/2$, with $z_i = (s^2/(a+b))((1+2w_1)(1+2w_r))^{-2^{i-1}}$, where $w_r = c/(a+b)$ and $w_1 = c_e/(a_e + b_e)$. The solution to u_i requires us to solve the following variant of the chaotic logistic map: $w_{i+1} = w_r + 2(1-2w_r)w_i(1-w_i)$, where $w_i = u_i/z_i$. We derive the exact solution of this quadratic recursion (see Supplementary Material for proof), and are thus able to evaluate $Q_i = [1 - t_d(1 - 2c_i/s_i)]/2$, which simplifies to the form shown in Theorem 1.

Even though our analysis assumed a deterministic entanglement source, it is easy to account for a probabilistic entanglement source with zero multi-pair emissions. Such a probabilistic entanglement source can be modeled as generating $|\psi\rangle = (1-p)|0\rangle\langle 0| + p|M^\pm\rangle\langle M^\pm|$ every T_q seconds. Since $|\psi\rangle$ can be regarded as the quantum state obtained by passing $|M^\pm\rangle$ through a beamsplitter of transmittance p , we can ‘push’ p through the BSM at the centers of elementary links, and apply our formulas after replacing $\lambda\eta_e$ by $\lambda\eta_e p$, and accordingly modifying the elementary link parameters: a_e, b_e, c_e .

Finally, even though all the above analysis was done for $N = 2^n$ elementary links (with n an integer), we believe that the final formula for Q and rate also hold for any integer N . In other words, with an end-to-end optical fiber channel with N elementary links,

$$R = \frac{P_1 P_{\text{succ}} R_2(Q(N))}{2T_q} \text{ secret-key bits/sec}, \quad (14)$$

where, $Q(N) = \frac{1}{2} \left[1 - (t_d/t_r) (t_r t_e)^N \right]$. Since $R(Q) = 1 - 2h_2(Q)$, with $h_2(x) = -x \log_2(x) - (1-x) \log_2(1-x)$ the binary entropy function, the maximum range for which QKD is possible at a nonzero rate is determined by when $Q(N)$ falls below Q_{th} , where $h_2(Q_{\text{th}}) = 1/2$. $Q_{\text{th}} \approx 0.1104$. One can invert $Q(N)$ to derive the maximum range as a function of number of elementary links N , and all the detector loss and noise parameters:

$$L_{\text{max}} = \frac{20N}{\alpha} \log_{10} \left[\frac{\eta_e}{8P_e} \left(\sqrt{8(1-2P_e)H} - 4(1-2P_e) \right) \right],$$

where $H = 1 + t_r / \left[(1 - 2Q_{\text{th}}) \frac{t_r}{t_d} \right]^{\frac{1}{N}}$ and α is the fiber loss coefficient, in dB/km.

NUMERICAL ANALYSIS

Main results.—Our main numerical results, described in detail in this section, are summarized below.

- 1. Quantum bosonic simulator.** We set up a full numerical simulation, using the sparse matrix toolbox of MATLAB to create time-efficient subroutines for beamsplitters, partial trace operations, and photon-number-resolving detectors, for efficiently simulating continuous-variable quantum dynamics on bosonic systems. This tool may find use in several future applications.
- 2. Verification of theory.** We use our tool to simulate the repeater-chain architecture described earlier in this paper, and evaluate secret-key rates as a function of distance. For an entanglement source with no 2 or higher-photon terms, the results from the theory and numerics are seen to match exactly.

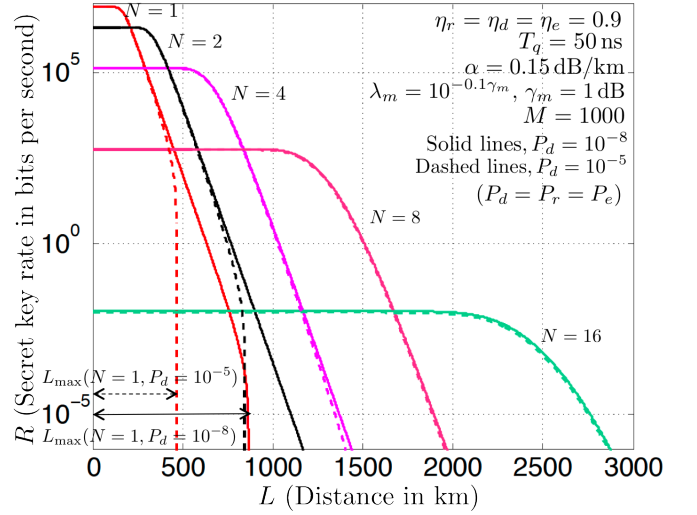


Figure 3. Secret key rate R as a function of range L , (theory and simulations match exactly), for ideal single-photon entanglement sources ($p(2) = 0$).

3. Sources with multi-pair emission. We analyze the performance of the architecture when the sources have non-zero two-pair emission rates ($g^2(0) > 0$). We find that the key rate quickly degrades with increasing two-pair probability, $p(2)$ of the source (see Fig. 4).

4. Error propagation. Our numerical simulations show that the scaling law in Eq. (4) we derived for error-propagation through the repeater chain holds—with an appropriate $p(2)$ -dependent modification to the pre-factor (t_r/t_d)—even for non-ideal sources (see Fig. 5(c)).

Detailed description of numerical results.—In Fig. 3, we plot the secret key rate as a function of range with $N = 2^n$ elementary links, with $n = 0, 1, \dots, 5$, for all system parameters held the same (see figure caption for the actual values used), but two different values of the dark-click probability of all the detectors in the system, $P_d = 10^{-5}$, and $P_d = 10^{-8}$. The first three plots ($N = 1, 2, 4$ elementary links) were computed both using the theoretical formula as well as the numerical simulation, and they match exactly. Following are key observations:

1. The envelope of the key rate (over all N) is close to identical for the two values of dark click probability. The maximum range L_{max} achievable by a given total number of elementary links, however, drastically decreases with increasing P_d .
2. At a given L , the range should be divided into an optimum number (N) of elementary links, to maximize the rate. At short distances, using too many repeaters diminishes the end-to-end key rate, due

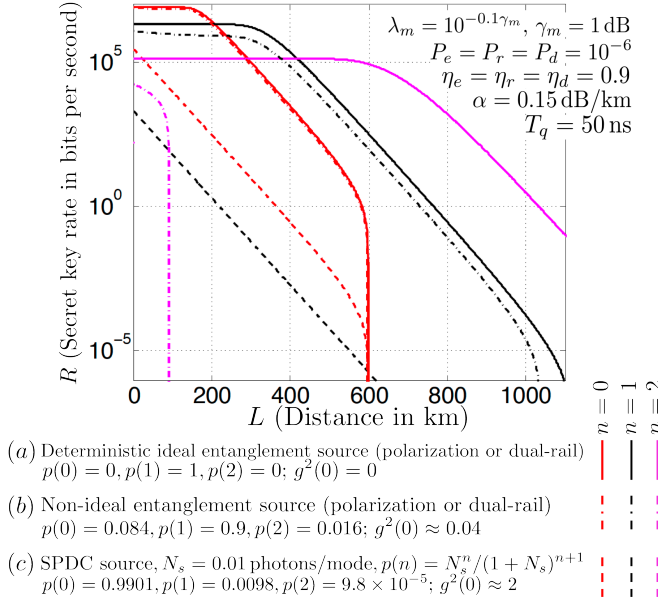


Figure 4. Secret key rate vs. distance compared for three sources: an ideal source, i.e., $g^2(0) = 0$, one with $g^2(0) \approx 0.04$, and one with $g^2(0) \approx 2$.

to the 50% heralding efficiencies of all the linear-optic BSMs at the elementary links and repeaters.

In Fig. 4, we plot the secret key rates for $N = 1, 2, 4$ elementary links ($n = 0, 1, 2$) with all parameters held constant, but for three choices of $p(1)$ and $p(2)$, the single-photon and two-pair probabilities of the entanglement source. We assume that the non-ideal source, instead of producing $|M^+\rangle = [|10, 01\rangle + |01, 10\rangle]/\sqrt{2}$, produces,

$$|\psi\rangle = \sqrt{1-p(1)-p(2)}|00, 00\rangle + \sqrt{p(1)}|M^+\rangle + \sqrt{p(2)/3}(|20, 02\rangle + |11, 11\rangle + |02, 20\rangle). \quad (15)$$

The reason we assume the above form is the following. One way to prepare $|M^+\rangle$ is to first create a pair of polarization-entangled photons, i.e., $(|H\rangle_1|V\rangle_2 + |V\rangle_1|H\rangle_2)/\sqrt{2}$, where $|H\rangle$ ($|V\rangle$) is a 1-photon Fock state in H (V) polarization, and 1 and 2 are spatial-mode labels. Passing both spatial modes of above through a pair of 50-50 beamsplitters generates the 2-photon 4-mode state $|M^+\rangle$. We assume that the multi-pair emission is symmetric in the two spatial modes, and that each spatial mode has exactly 2 photons each, to the leading order. If $p(2)$ is small, the exact form of the two-pair term does not seem to affect the results, notwithstanding that our simulation is easily able to take into account any particular form of the two-pair term, depending upon the physical model of the actual source. The key observations from Fig. 4 are as follows [21]:

1. For a slightly non-ideal source (i.e., $p(0) = 0.084$, $p(1) = 0.9$, $p(2) = 0.016$), with $g^2(0) \approx 0.04$, the key rate with one elementary link remains almost

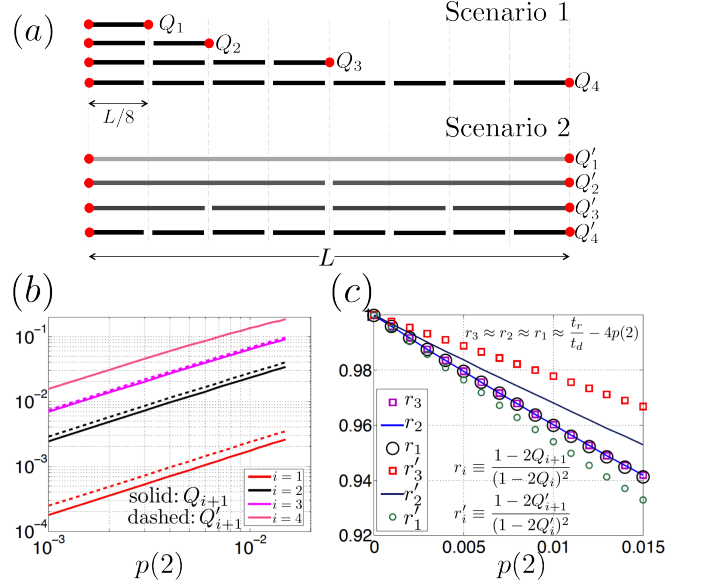


Figure 5. QBER vs. $p(2)$, for different numbers of swaps at a fixed distance of $L = 50$ km, for two different ways to incrementally arriving at the $N = 2^3$ elementary-link construction. We assume, $\eta_e = \eta_r = \eta_d = 0.9$, $P_e = P_r = P_d = 10^{-6}$, $M = 1000$, $\alpha = 0.15$ dB/km, $\lambda_m = 1$ dB, and $T_q = 50$ ns.

the same as that of the ideal source for all range values. With the range split into 2 elementary links, the rate drops a little compared to the ideal source. With 4 or more elementary links, the rate becomes abysmally small, smaller even than the rate attained by a single elementary link.

2. With an SPDC source statistics, i.e., $p(n) = N_s^n / (1 + N_s)^{n+1}$ for $n = 0, 1$, with $N_s = 0.01$, and $p(2) = 1 - p(0) - p(1)$, with one elementary link, the rate is much worse compared to the ideal source. With 2 elementary links, the rate drops below what is achieved with one link for most of the range, and with 4 or higher elementary links, $Q(N)$ never crosses below Q_{th} , and the rate is always zero. An intuitive way to understand this is as follows. For $N_s \ll 1$, $p(2) \approx p(1)^2$, which means that the probability of single-pair terms from two copies of (15) to interfere at the BSM is comparable to the probability that a two-pair term from one side interferes with the vacuum term from the other, where the latter causes an erroneous post-selection event.

In Fig. 5(a), we depict two ways to incrementally arrive at the L -km-range, $N = 2^n$ elementary-link construction, for $n = 3$. Scenario 1 is the one considered in our theoretical development, where the Alice-to-Bob range L is divided up into $N = 2^n$ elementary links, and Q_i is defined as the error probability if Alice and Bob were to measure the state ρ_i (which is formed after successfully

connecting 2^{i-1} elementary links), $1 \leq i \leq n+1$. In Scenario 2, we divide up the entire range L into 2^{i-1} elementary links, and conditioned on successfully connecting them, we define Q'_i as the error probability on the sifted raw bit when Alice and Bob make a measurement on the L -km-range connected link ρ'_i , in the same bases.

In Fig. 5(b), we plot Q_i and Q'_i as a function of $p(2)$, when $p(1) = 0.9$ is held fixed, with $p(0) = 1 - p(1) - p(2)$, for $N = 2^n$, with $n = 3$. Clearly, $Q_4 = Q'_4$, as for $i = n+1$, the two scenarios are identical. Furthermore, $Q'_i > Q_i$ for $1 \leq i \leq n$, since the measurement is made over the same number (2^{i-1}) of elementary links, but the elementary links are longer (and hence noisier) in Scenario 2. The QBER seems to grow almost linearly with $p(2)$, for the chosen system parameters.

In Fig. 5(c), we plot $(1 - 2Q_{i+1})/(1 - 2Q_i)^2$ for $i = 1, 2, 3$, as a function of $p(2)$. For the ideal source ($p(2) = 0$), we proved that this ratio (t_r/t_d) should be independent of i (4). For the chosen loss and noise parameters, $t_r/t_d = 1 - \epsilon$, with $\epsilon = 1.39 \times 10^{-5}$. We find that the ratio is independent of i , also for the imperfect source, at all values of $p(2) \in [0, 0.015]$. The ratio has an excellent fit with $(t_r/t_d) - 4p(2)$. This is very interesting, as it gives us a way to calculate the QBER on long repeater chains by making a physical measurement on one noisy elementary link. On the other hand, the ratio $(1 - 2Q'_{i+1})/(1 - 2Q'_i)^2$ for $i = 1, 2, 3$, increases with i , but each seem to also decay linearly with $p(2)$.

CONCLUSIONS

Long-distance entanglement distribution at high rates is of paramount importance to many quantum communication protocols, to realize which one must build a chain of quantum repeaters. Several quantum repeater protocols have been proposed [7–10, 12], all of which use some source of entanglement, some form of quantum memories, and linear-optics-based Bell-state measurement. We analyzed the architecture proposed in [12], which is a repeater protocol that has a superior classical communication overhead, and does not rely on purification of noisy shared entangled pairs. Our analysis easily carries over to other repeater architectures.

We solved exactly for the quantum state after a given number of swaps in a concatenated quantum-repeater chain that uses heralded linear-optic Bell-state measurements (BSM). We exploit the fact that if we start with a single-photon entanglement source, the post-selected state after a successful BSM remains in a subspace spanned by the single photon terms, and recursively evaluate the state using an exact model for the imperfect single-photon detectors. This calculation required us to exactly solve a variant of the logistic map from chaos theory. Using this expression for the quantum state, we determined quantities such as the success probability of

entanglement swapping at any given swap level, the error rate of the raw bits obtained by Alice and Bob in a QKD application if they were to measure this state in the same bases, and the sifting probability. One can find any other quantity of interest from the state, such as the entanglement of formation or the fidelity with the maximally entangled state (which is done in the Supplementary Material). Our analysis takes into account all major imperfections of the detectors (such as detection efficiencies, and dark click probabilities) and the channel (such as transmissivity and thermal noise, where the latter can be included into an effective dark-click probability term). We also evaluate an exact scaling law for how the quantum bit error rate (QBER) evolves from one swap level to the next, which we found to hold also when the entanglement source is imperfect. This is of great practical importance since it gives us a way to calculate the QBER on long repeater chains by making a physical measurement on one noisy elementary link. Next, we simulated the repeater-chain architecture, and the QKD protocol numerically, using a new efficient model we developed for simulating bosonic states, unitaries, and measurements. We noticed that when the two photon probability $p(2)$ increases, the key rates drastically fall to zero (instead of becoming higher) when adding elementary links to the system.

One can in principle replace the linear-optic entanglement swapping scheme with more advanced schemes with improved heralding efficiencies, such as the one proposed by Grice [22] that injects entangled states into a beam-splitter network and heralds total number of clicks from an array of photon-number-resolving detectors. Yet another improved BSM was proposed recently that uses inline squeezers to beat the 50%-efficiency limit of a linear-optic BSM [23]. Our theoretical technique can be readily used to analyze the repeater-chain architecture when the BSMs are replaced by one of the aforesaid schemes. At each swap stage, after the post-selection by the BSM, the projected shared state will still lie in the span of the 4-mode 2-qubit dual-rail basis, but there will be two extra coefficients to track, since the advanced BSMs can identify all four Bell states (as opposed to only two by the linear-optic scheme [14]). It is quite likely that the final expression for Q_i , and the error-propagation law will still depend upon t_d , t_r , and t_e , where the latter two are the same functions of the fractional probability transfer to classical correlations at each swap stage (which should be smaller compared to when the linear-optic BSM is used). Finally, our numerical model allows us to simulate these enhanced schemes as well, and also introduce other non-idealities such as finite memory times at the repeaters, non-linearities in the fiber and memories, and timing jitter at detectors. The analysis of the repeater chain with the advanced BSM schemes is left for future work.

The authors would like to thank Wolfgang Tittel, Christoph Simon, Khabat Heshami, Joshua Slater, Gregory Kanter and Yuping Huang for useful discussions. This paper is based on research funded by the DARPA Quiness program subaward contract number SP0020412-PROJ0005188, under prime contract number W31P4Q-13-1-0004. The views and conclusions contained in this document are those of the authors and should not be interpreted as representing the official policies, either expressly or implied, of the Defense Advanced Research Projects Agency or the U.S. Government.

Y.-P. Huang, C. Thiel, *to be published*, Proceedings of the Conference on Lasers and Electro-Optics (CLEO), June 8-13, San Jose, CA, (2014).

[22] W. P. Grice, Phys. Rev. A **84**, 042331 (2011).

[23] H. A. Zaidi and P. van Loock, Phys. Rev. Lett. **110**, 260501 (2013).

-
- [1] A. Ekert, Phys. Rev. Lett. **67**, 6 (1991).
 - [2] C. H. Bennett, G. Brassard, C. Crépeau, R. Jozsa, A. Peres, and W. K. Wootters, Phys. Rev. Lett. **70**, 1895–1899 (1993).
 - [3] C. Bennett and S.J. Wiesner, Phys. Rev. Lett. **69**, 2881 (1992).
 - [4] M. M. Wilde and M.-H. Hsieh, Quantum Information Processing **11**, 6, 1431–1463, (2012).
 - [5] M. M. Wilde, P. Hayden, and S. Guha, Phys. Rev. Lett. **108**, 140501 (2012).
 - [6] M. Takeoka, S. Guha, and M. M. Wilde, arXiv:1310.0129 [quant-ph] (2013).
 - [7] N. Sangouard, C. Simon, H. de Riedmatten, and N. Gisin, Rev. Mod. Phys. **83**, 33 (2011).
 - [8] H.-J. Briegel, W. Dür, J. I. Cirac, and P. Zoller, Phys. Rev. Lett. **81**, 5932 (1998).
 - [9] L.-M. Duan, M. D. Lukin, J. I. Cirac, and P. Zoller, Nature **414**, 413–418, 22 November (2001).
 - [10] L. Jiang, J. M. Taylor, K. Nemoto, W. J. Munro, R. V. Meter, and M. D. Lukin, Phys. Rev. A **79**, 032325, (2009).
 - [11] S. Bratzik, H. Kampermann, and D. Bruß, Phys. Rev. A **89**, 032335 (2014).
 - [12] N. Sinclair, E. Saglamyurek, H. Mallazadeh, J.A. Slater, M. Hedges, M. George, R. Ricken, D. Oblak, W. Sohler, and W. Tittel, <http://arxiv.org/abs/1309.3202>.
 - [13] S. L. Braunstein, and A. Mann, Phys. Rev. A *Rapid Communications*, **51**, 3 (1995).
 - [14] N. Lütkenhaus, J. Calsamiglia, and K.-A. Suominen, Phys. Rev. A **59**, 3295 (1999).
 - [15] A. Khalique, W. Tittel, and B. C. Sanders, Phys. Rev. A **88**, 022336 (2013).
 - [16] M. Razavi, H. Farmanbar, and N. Lütkenhaus, Optical Fiber Communication (OFC) Conference, San Diego, California, United States, February 24-28, (2008).
 - [17] E. Schröder, “Über iterierte Funktionen”, Math. Ann. **3** (2): 296–322, doi:10.1007/BF01443992 (1870).
 - [18] E. Saglamyurek, N. Sinclair, J. Jin, J. A. Slater, D. Oblak, F. Bussi eres, M. George, R. Ricken, W. Sohler, W. Tittel, Nature **469**, 512 (2011).
 - [19] A. Ferenczi and N. Lütkenhaus, Phys. Rev. A **85**, 052310 (2012).
 - [20] Zhao-Xi Xiong, Han-Duo Shi, Yi-Nan Wang, Li Jing, Jin Lei, Liang-Zhu Mu and Heng Fan, Phys. Rev. A, **85**, 012334 (2012).
 - [21] H. Krovi, Z. Dutton, S. Guha, C. A. Fuchs, W. Tittel, C. Simon, J. Slater, K. Heshami, M. Hedges, G. S. Kanter,

Supplemental Material: Exact analysis of long distance quantum communication using concatenated entanglement swapping with noisy detectors and sources

PROOF OF PROPOSITION 2: QUANTUM STATE OF THE ELEMENTARY LINK, AND CONNECTIONS THROUGH SWAP STAGES

Elementary link

We first prove Proposition 2 for the case $i = 1$, and derive the post-selected quantum state of the elementary link. Let us first consider how we should model nonideal photodetectors. Ideally we would like to say that each of the four detectors required for the BSM individually measures a Hermitian operator with eigen-projectors $\{\Pi_0, \Pi_1, \Pi_2\}$, the $\Pi_n = |n\rangle\langle n|$ signifying the presence of n photons. Next we note that we are allowed to limit ourselves to a three-dimensional subspace of the Fock space because we know we will never have more than two photons at a detection site (since we limit the theoretical part of analysis to the case when the sources have $g^2(0) = 0$ and assume that any thermal noise in the channel is negligible at typical optical frequencies). The detectors are assumed to have a sub-unity detection efficiency η_e —which may be thought of as arising from a beamsplitter with transmittivity $\sqrt{\eta_e}$ just in front of an ideal detector—and independently there may also be a probability P_e for the detector to trigger in the absence of a photon. This means the “no click” and “click” events in the individual detectors really correspond to a two-outcome POVM $\{F_0, F_1\}$, with

$$F_0 = (1 - P_e)\Pi_0 + (1 - A_e)\Pi_1 + (1 - B_e)\Pi_2 \quad (S1)$$

$$F_1 = P_e\Pi_0 + A_e\Pi_1 + B_e\Pi_2. \quad (S2)$$

where we take

$$A_e = 1 - (1 - P_e)(1 - \eta) \quad (S3)$$

$$B_e = 1 - (1 - P_e)(1 - \eta)^2. \quad (S4)$$

The way to understand F_0 , the “no click” signal for instance, is this: If there are no actual photons present, one will get this outcome with probability $1 - P_e$, the probability for no false alarm at the detector. On the other hand, if there is a single photon present both it must disappear and there still be no false alarm; hence a coefficient $(1 - P_e)(1 - \eta)$ in front of Π_1 . Finally, for the case that two photons are present, both of them must be lost and yet no false alarm must appear; hence a coefficient of $(1 - P_e)(1 - \eta)^2$.

We next note that we may incorporate the channel transmittance λ (corresponding to propagation loss of each of the halves of the Bell pairs from two ends of the elementary link) directly into the detection efficiency η_e , by defining an effective detection efficiency $\eta_e\lambda$ while assuming the channel is lossless, rather than accounting for the channel loss in our description of the quantum states arriving at them. One can see this through a simple bosonic mode-operator analysis including two stages of loss, but the intuition should be clear. Consequently, at the center of an elementary link we can assume the state it will attempt to link is a clean $|M^+\rangle|M^+\rangle$, while the four detectors in the BSM are working at efficiency

$$\eta = \eta_e\lambda. \quad (S5)$$

This greatly simplifies the analysis by not having to treat the states to be linked as mixed states.

For the purposes of this proof, let us label the four spatial modes involved in an elementary link by a , b , c , and d , so that the initial quantum state is more explicitly $|M_{ab}^+\rangle|M_{cd}^+\rangle$. The BSM will be applied to modes b and c . What this entails is that the modes first impinge on a 50-50 beamsplitter, which enacts a mode transformation

$$b_j^\dagger \longrightarrow \sqrt{\frac{1}{2}}(b_j^\dagger + c_j^\dagger) \quad \text{and} \quad c_j^\dagger \longrightarrow \sqrt{\frac{1}{2}}(b_j^\dagger - c_j^\dagger). \quad (S6)$$

The consequence of this is that the state presented to the photo detectors is a massively entangled one:

$$\begin{aligned} |\text{swap}\rangle = \frac{1}{4} \big(& |10, 11, 00, 01\rangle - |10, 01, 10, 01\rangle + \sqrt{2}|10, 02, 00, 10\rangle + |10, 10, 01, 01\rangle \\ & - |10, 00, 11, 01\rangle - \sqrt{2}|10, 00, 02, 10\rangle + \sqrt{2}|01, 20, 00, 01\rangle + |01, 11, 00, 10\rangle \\ & - |01, 10, 01, 10\rangle - \sqrt{2}|01, 00, 20, 01\rangle + |01, 01, 10, 10\rangle - |01, 00, 11, 10\rangle \big) \end{aligned} \quad (S7)$$

Ideally then, if one were to obtain a 1-2 coincidence or a 3-4 coincidence in the detectors at the four dual-rail modes, a successful entanglement swap would be declared and a new state $|M_{ad}^+\rangle$ would be ascribed to the photons in quantum memory. However with noisy detectors, one should use Lüders' rule for the POVM above to get the new state. For instance, suppose we were to detect a 1-2 coincidence in the detectors. Then, this is signified by the POVM element

$$F_1 \otimes F_1 \otimes F_0 \otimes F_0 = P_e^2(1 - P_e^2)^2 \Pi_0 \otimes \Pi_0 \otimes \Pi_0 \otimes \Pi_0 + P_e^2(1 - P_e^2)(1 - A_e) \Pi_0 \otimes \Pi_0 \otimes \Pi_0 \otimes \Pi_1 + \text{etc.} \quad (\text{S8})$$

and the new state for the a - d system will be

$$\rho'_{ad} = \frac{1}{\text{Prob}(F_1 \otimes F_1 \otimes F_0 \otimes F_0)} \text{tr}_{bc} \left(\sqrt{F_1 \otimes F_1 \otimes F_0 \otimes F_0} |\text{swap}\rangle \langle \text{swap}| \sqrt{F_1 \otimes F_1 \otimes F_0 \otimes F_0} \right). \quad (\text{S9})$$

From here it out is just a question of brute-force calculation. At the end of it, one finds:

$$\begin{aligned} \rho'_{ad} = \frac{1}{8s_1} \left\{ \left[A_e^2(1 - P_e)^2 + P_e^2(1 - A_e)^2 \right] |M_{ad}^+\rangle \langle M_{ad}^+| + 2A_e P_e(1 - A_e)(1 - P_e) |M_{ad}^-\rangle \langle M_{ad}^-| \right. \\ \left. + P_e(1 - P_e) \left[P_e(1 - B_e) + B_e(1 - P_e) \right] \left(|01, 01\rangle \langle 01, 01| + |10, 10\rangle \langle 10, 10| \right) \right\}, \end{aligned} \quad (\text{S10})$$

where

$$s_1 = \frac{1}{8} \left[(A_e + P_e - 2A_e P_e)^2 + P_e(1 - P_e)(B_e + P_e - 2B_e P_e) \right]. \quad (\text{S11})$$

Thus one has mostly the swap expected. But with some probability one gets an unexpected swap, and with some probability an induced classical correlation between the photons in the memory. By symmetry one has the same result for a 3-4 coincidence, and for 1-4 and 2-3 coincidences, one just interchanges the roles of $|M_{ad}^+\rangle$ and $|M_{ad}^-\rangle$ in this expression. We therefore have the state of an elementary link given by:

$$\rho_1 = \frac{1}{s_1} \left[a_1 |M^+\rangle \langle M^+| + b_1 |M^-\rangle \langle M^-| + c_1 |\psi_0\rangle \langle \psi_0| + d_1 |\psi_1\rangle \langle \psi_1| + d_1 |\psi_2\rangle \langle \psi_2| + c_1 |\psi_3\rangle \langle \psi_3| \right], \quad (\text{S12})$$

where $|\psi_0\rangle = |01, 01\rangle$, $|\psi_1\rangle = |01, 10\rangle$, $|\psi_2\rangle = |10, 01\rangle$, $|\psi_3\rangle = |10, 10\rangle$, $|M^\pm\rangle = [|\psi_2\rangle \pm |\psi_1\rangle] / \sqrt{2}$, $s_1 = a_1 + b_1 + 2(c_1 + d_1)$ is a normalization constant, and the coefficients a_1 , b_1 , c_1 , d_1 are given by:

$$a_1 \equiv a_e = \frac{1}{8} \left[P_e^2(1 - A_e)^2 + A_e^2(1 - P_e)^2 \right], \quad (\text{S13})$$

$$b_1 \equiv b_e = \frac{1}{8} \left[2A_e P_e(1 - A_e)(1 - P_e) \right], \quad (\text{S14})$$

$$c_1 \equiv c_e = \frac{1}{8} P_e(1 - P_e) \left[P_e(1 - B_e) + B_e(1 - P_e) \right], \quad (\text{S15})$$

$$d_1 \equiv d_e = 0, \quad (\text{S16})$$

where $A_e = \eta_e \lambda + P_e(1 - \eta_e \lambda)$ and $B_e = 1 - (1 - P_e)(1 - \eta_e \lambda)^2$.

Connections through swap stages at the quantum repeater nodes

Next we consider the case $i \geq 2$. The proof proceeds as follows. We first realize, by term-by-term evaluation of connecting two copies of ρ_1 , that the state ρ_i never goes outside the span of $|\psi_0\rangle, |\psi_1\rangle, |\psi_2\rangle, |\psi_3\rangle$. It is convenient to express the state ρ_i as:

$$\rho_i = \frac{1}{s_i} \left[r_1^{(i)} |M^+\rangle \langle M^+| + r_2^{(i)} |M^-\rangle \langle M^-| + r_3^{(i)} |\psi_0\rangle \langle \psi_0| + r_4^{(i)} |\psi_1\rangle \langle \psi_1| + r_5^{(i)} |\psi_2\rangle \langle \psi_2| + r_6^{(i)} |\psi_3\rangle \langle \psi_3| \right], \quad (\text{S17})$$

where $s_i = \sum_{l=1}^6 r_l^{(i)}$. Then, we realize that each subsequent connection evolves the state as,

$$r_l^{(i+1)} = \sum_{j=1}^6 \sum_{k=1}^6 C_{j,k,l} r_j^{(i)} r_k^{(i)}, \quad (\text{S18})$$

with the matrix C given by (each term of which is calculated by brute-force algebra):

$$\begin{aligned}
C(1, 1, :) &= [a, b, c, 0, 0, c] \\
C(1, 2, :) &= [b, a, c, 0, 0, c] \\
C(1, 3, :) &= [0, 0, a + b, 0, 2c, 0] \\
C(1, 4, :) &= [0, 0, 0, a + b, 0, 2c] \\
C(1, 5, :) &= [0, 0, 2c, 0, a + b, 0] \\
C(1, 6, :) &= [0, 0, 0, 2c, 0, a + b], \\
\\
C(2, 1, :) &= [a, b, c, 0, 0, c] \\
C(2, 2, :) &= [b, a, c, 0, 0, c] \\
C(2, 3, :) &= [0, 0, a + b, 0, 2c, 0] \\
C(2, 4, :) &= [0, 0, 0, a + b, 0, 2c] \\
C(2, 5, :) &= [0, 0, 2c, 0, a + b, 0] \\
C(2, 6, :) &= [0, 0, 0, 2c, 0, a + b], \\
\\
C(3, 1, :) &= [0, 0, a + b, 2c, 0, 0] \\
C(3, 2, :) &= [0, 0, a + b, 2c, 0, 0] \\
C(3, 3, :) &= [0, 0, 4c, 0, 0, 0] \\
C(3, 4, :) &= [0, 0, 0, 4c, 0, 0] \\
C(3, 5, :) &= [0, 0, 2(a + b), 0, 0, 0] \\
C(3, 6, :) &= [0, 0, 0, 2(a + b), 0, 0], \\
\\
C(4, 1, :) &= [0, 0, 2c, a + b, 0, 0] \\
C(4, 2, :) &= [0, 0, 2c, a + b, 0, 0] \\
C(4, 3, :) &= [0, 0, 2(a + b), 0, 0, 0] \\
C(4, 4, :) &= [0, 0, 0, 2(a + b), 0, 0] \\
C(4, 5, :) &= [0, 0, 4c, 0, 0, 0] \\
C(4, 6, :) &= [0, 0, 0, 4c, 0, 0], \\
\\
C(5, 1, :) &= [0, 0, 0, 0, a + b, 2c] \\
C(5, 2, :) &= [0, 0, 0, 0, a + b, 2c] \\
C(5, 3, :) &= [0, 0, 0, 0, 4c, 0] \\
C(5, 4, :) &= [0, 0, 0, 0, 0, 4c] \\
C(5, 5, :) &= [0, 0, 0, 0, 2(a + b), 0] \\
C(5, 6, :) &= [0, 0, 0, 0, 0, 2(a + b)], \\
\\
C(6, 1, :) &= [0, 0, 0, 0, 2c, a + b] \\
C(6, 2, :) &= [0, 0, 0, 0, 2c, a + b] \\
C(6, 3, :) &= [0, 0, 0, 0, 2(a + b), 0] \\
C(6, 4, :) &= [0, 0, 0, 0, 0, 2(a + b)] \\
C(6, 5, :) &= [0, 0, 0, 0, 4c, 0] \\
C(6, 6, :) &= [0, 0, 0, 0, 0, 4c], \tag{S19}
\end{aligned}$$

where the “:” sign indicates all entries $C(j, k, l)$ for $1 \leq l \leq 6$. The rest is just writing out $r_l^{(i+1)}$ explicitly, and realizing that,

$$r_3^{(i)} = r_6^{(i)}, \text{ and} \tag{S20}$$

$$r_4^{(i)} = r_5^{(i)}, \tag{S21}$$

and hence the fact that we can rename the coefficients as: $r_1^{(i)} = a_i, r_2^{(i)} = b_i, r_3^{(i)} = r_6^{(i)} = c_i$, and $r_4^{(i)} = r_5^{(i)} = d_i$.

EVALUATING THE SUCCESS PROBABILITIES

It is easy to realize from the derivation of the states ρ_i that the success probability (to connect two copies of ρ_{i-1} to obtain one copy of ρ_i) is simply given by $P_s(i) = 4s_i$, for $i \geq 2$. The probability an elementary link is successfully created is $P_s(1) = 1 - (1 - P_{s0})^M$, where $P_{s0} = 4s_1$ is the probability of successful creation of an elementary link ρ_1 in one of the M frequencies at the center of the elementary link, where $s_1 = a_e + b_e + 2c_e$. It is simple now to calculate the success probabilities $P_s(i)$ by proving that $s_i = s$, $\forall i \geq 2$. We thus have the following proposition.

Proposition 3 *The success probability of connecting two copies of ρ_{i-1} to produce a usable copy of ρ_i , $P_s(i) = 4s_i$, where*

$$s_i = a + b + 2c \triangleq s, \quad 2 \leq i \leq n + 1. \quad (\text{S22})$$

Proof. Denoting $x_i = a_i + b_i + c_i + d_i$, and $y_i = c_i + d_i$, using Eqs. (6), (7), (8), (9), we have,

$$x_{i+1} = \frac{1}{s_i^2} [(a + b + c)(x_i^2 + y_i^2) + 2cx_iy_i], \quad (\text{S23})$$

$$y_{i+1} = \frac{1}{s_i^2} [c(x_i - y_i)^2 + 2(a + b + 2c)x_iy_i], \quad (\text{S24})$$

with $s_i = x_i + y_i$ by definition. It is easy to now see that $x_{i+1} + y_{i+1} = a + b + 2c \equiv s$, for all $i \in \{2, 3, \dots, n + 1\}$. Note that $P_s(1) = 1 - (1 - 4s_1)^M$, with $s_1 = a_e + b_e + 2c_e$ for the elementary link. ■

EVALUATING THE SIFT PROBABILITY

In this section, we derive P_1 , the probability that Alice and Bob both get exactly one click each, i.e., they decide to use their click outcomes for further processing to extract a key when they measure their halves of the shared entangled state ρ_{n+1} , after $N = 2^n$ elementary links have been connected successfully.

Let us first assume Alice and Bob share the state ρ_i , and they make a measurement (in the same basis). We proceed as follows.

Proposition 4 *Let P_1 denote the probability that Alice and Bob both get exactly one click each, i.e., they decide to use their click outcomes for further processing to extract a key. It is straightforward to argue that, regardless of the value of i ,*

$$P_1 = (q_1 + q_2)^2, \quad (\text{S25})$$

where $q_1 = (1 - P_d)A_d$, $q_2 = (1 - A_d)P_d$, with $A_d = \eta_d P_d + 1 - \eta_d$ are loss and noise parameters of Alice's and Bob's single-photon detectors.

Proof. This can be proven rigorously by simply evaluating $\text{Tr}[\rho_i(M_{0101} + M_{0110} + M_{1001} + M_{1010})]$, where $M_{ijkl} \equiv F_i \otimes F_j \otimes F_k \otimes F_l$, with the POVM elements of a lossy-noisy single-photon detector POVMs F_0 and F_1 defined above. Here we will sketch a more intuitive (but less rigorous) proof. Note that $\rho_i \in \text{span}(|\psi_0\rangle, |\psi_1\rangle, |\psi_2\rangle, |\psi_3\rangle)$, with $|\psi_0\rangle = |01, 01\rangle$, $|\psi_1\rangle = |01, 10\rangle$, $|\psi_2\rangle = |10, 01\rangle$, $|\psi_3\rangle = |10, 10\rangle$, since $|M^\pm\rangle = [|\psi_2\rangle \pm |\psi_1\rangle]/\sqrt{2}$. Therefore, Alice's and Bob's reduced density operators always have exactly one photon in one of two modes. Let us define $q_1 \triangleq P[\text{noflip}]$ to be the probability that a $|01\rangle$ state is detected as “(0, 1)” by the lossy-noisy detector, where (0, 1) stands for (no-click, click). Clearly, q_1 is also the probability that $|10\rangle$ is detected as “(1, 0)”. In order for “no flip” to happen, no dark click should appear in the mode in the vacuum state (this happens with probability P_d), and that the photon in the other mode should either be detected by the lossy detector (happens with probability $1 - \eta_d$, in which case it does not matter whether or not a dark click appears), or the photon does not get detected, and a dark click appears (which happens with probability $\eta_d P_d$). Therefore, $q_1 = (1 - P_d)A_d$, with $A_d = \eta_d P_d + 1 - \eta_d$. Similarly, we define $q_2 \triangleq P[\text{flip}]$ to be the probability that $|01\rangle$ is detected as “(1, 0)” (or, $|10\rangle$ is detected as “(0, 1)”). For a “flip” event to happen, a dark click should appear in the vacuum mode (probability P_d), and the photon containing mode should not be detected and a dark click must not appear (happens with probability, $\eta_d(1 - P_d)$). Therefore, $q_2 = (\eta_d(1 - P_d))P_d = (1 - A_d)P_d$. Clearly, $q_1 + q_2$ need not add up to 1 in general, since the detectors may output “(0, 0)” or “(1, 1)” outcomes, which are not used by Alice and Bob. Therefore $(q_1 + q_2)^2$ is the probability that Alice and Bob obtain a *usable* detection outcome, i.e., both of them collectively obtain one of the four outcomes: (0, 1; 0, 1), (0, 1; 1, 0), (1, 0; 0, 1), (1, 0; 1, 0). This is true regardless of the actual fraction of $|10\rangle$ and $|01\rangle$ in Alice's and Bob's states. Hence, $P_1 = (q_1 + q_2)^2$. ■

EVALUATING THE QBER AND SECRET KEY RATES

In this section, we will evaluate the explicit formula for Q_i , the quantum bit-error rate (QBER), which is the probability that Alice and Bob obtain a mismatched raw key bit, despite the fact that they make measurements in the same bases on a successfully-created copy of ρ_i , and that they both get exactly single-clicks (on the two modes of their respective qubits). The first step in doing so is to solve for the quantum state ρ_i more explicitly than what the recursions in Proposition 2 give us.

Explicit solution for the quantum state, ρ_i

Recall that we proved above that $s_i = a + b + 2c \triangleq s$, $2 \leq i \leq n + 1$, by defining $x_i = a_i + b_i + c_i + d_i$, and $y_i = c_i + d_i$, and using Eqs. (6), (7), (8), (9), to obtain $x_{i+1} + y_{i+1} = a + b + 2c \equiv s$, for all $i \in \{2, 3, \dots, n + 1\}$, and that $s_1 = a_e + b_e + 2c_e$ for the elementary link. Let us now proceed to calculate the coefficients a_i , b_i , c_i and d_i , all explicitly as a function of i , $1 \leq i \leq n + 1$, and the system's loss and noise parameters.

Proposition 5 $a_i + b_i \equiv z_i$ is given by,

$$z_i = \nu \left(\frac{z_1}{\nu} \times \frac{s}{s_1} \right)^{2^{i-1}}, \quad i \geq 2, \quad (\text{S26})$$

where $z_1 = a_e + b_e$, $s_1 = a_e + b_e + 2c_e$, $\nu = s^2/(a + b)$, and $s \triangleq s_i$, for $i \geq 2$.

Proof. The proof follows by realizing that with the definitions in Eqs. (S23) and (S24), $x_i - y_i = a_i + b_i$, and,

$$x_{i+1} - y_{i+1} = \frac{1}{s_i^2} (a + b) (x_i - y_i)^2. \quad (\text{S27})$$

■

Remark 6 Note that since $x_i + y_i = s_i$, and $x_i - y_i = z_i$, we have,

$$y_i = c_i + d_i = \frac{1}{2} \left[s_i - \nu \left(\frac{s z_1}{s_1 \nu} \right)^{2^{i-1}} \right]. \quad (\text{S28})$$

As we will see in the next subsection, the error probability Q_i depends only on $2c_i/s_i$ —the fractional probability of the classical correlations when two copies of ρ_{i-1} are connected. Note that $(a_i + b_i)$ is the sum fractional probability of the Bell states $|M^+\rangle$ (a_i) and $|M^-\rangle$ (b_i) when two copies of ρ_{i-1} are connected, and $s_i = (a_i + b_i) + 2c_i$. Since we already have $c_i + d_i$ explicitly available, let us calculate $c_i - d_i \equiv u_i$.

Proposition 7 The difference $c_i - d_i \equiv u_i$ can be found as the solution to the following quadratic difference equation,

$$w_{i+1} = w_r + 2(1 - 2w_r)w_i(1 - w_i), \quad (\text{S29})$$

where $w_i \triangleq u_i/z_i$, $w_r = c/(a + b)$, and $w_1 = c_e/(a_e + b_e)$.

Proof. The proof follows from simply writing down $c_{i+1} - d_{i+1}$ using Eqs. (8) and (9), substituting $w_i = u_i/z_i$, and simplifying. ■

Remark 8 The difference equation (S29) reduces to the famous Logistic Map, when $w_r = 0$. The solution to the logistic map $w_{i+1} = R w_i(1 - w_i)$, $w_i \in (0, 1)$, is in general chaotic, but for $R = 2$ (which is exactly what (S29) reduces to when $w_r = 0$) was found exactly by Ernst Schröder in 1870, as:

$$w_i = \frac{1}{2} \left[1 - (1 - 2w_1)^{2^{i-1}} \right]. \quad (\text{S30})$$

Theorem 9 The quadratic difference equation, $w_{i+1} = w_r + 2(1 - 2w_r)w_i(1 - w_i)$, which is a variant of the logistic map $w_{i+1} = 2w_i(1 - w_i)$ with $R = 2$, can be exactly solved, and the solution is given by:

$$w_i = \frac{1}{2} \left[1 - \frac{1}{\beta} [\beta(1 - 2w_1)]^{2^{i-1}} \right], \quad (\text{S31})$$

where $\beta = 1 - 2w_r$. This correctly reduces to (S30) when $w_r = 0$.

Proof. See next Section for the proof. ■

Next, we find c_i . We add the following two expressions:

$$c_i + d_i = (s_i - z_i)/2, \text{ and} \quad (\text{S32})$$

$$c_i - d_i = u_i = \frac{z_i}{2} \left[1 - \frac{1}{\beta} [\beta(1 - 2w_1)]^{2^{i-1}} \right], \quad (\text{S33})$$

and divide by 2, to obtain:

$$c_i = \frac{s_i}{4} \left[1 - \frac{z_i}{\beta s_i} [\beta(1 - 2w_1)]^{2^{i-1}} \right]. \quad (\text{S34})$$

At this point, since we have c_i , it is sufficient to calculate Q_i (see next subsection). However, let us go ahead and evaluate a_i and b_i as well, so that we have a complete characterization of the quantum state ρ_i , which can be used to calculate other quantities of interest, such as the fidelity, entanglement of formation, etc.

Since we already have $a_i + b_i = z_i$ from Proposition 5, we need to calculate $a_i - b_i$.

Proposition 10 $a_i - b_i \equiv v_i$ is given by the following recursion,

$$v_i = \frac{1}{s_i^2} (a - b) z_i v_i, \quad (\text{S35})$$

which can be solved to obtain:

$$v_i = \left(\frac{a - b}{a + b} \right)^{i-1} \left(\frac{a_e - b_e}{a_e + b_e} \right) z_i, \quad (\text{S36})$$

where z_i is given by Eq. (S26).

Proof. The proof follows simply by subtracting the expressions for b_{i+1} from that of a_{i+1} , given in Proposition 2, and simplifying. ■

With that, we finally have the state ρ_i as,

$$\rho_i = \frac{1}{s_i} [a_i |M^+\rangle \langle M^+| + b_i |M^-\rangle \langle M^-| + c_i |\psi_0\rangle \langle \psi_0| + d_i |\psi_1\rangle \langle \psi_1| + d_i |\psi_2\rangle \langle \psi_2| + c_i |\psi_3\rangle \langle \psi_3|], \quad (\text{S37})$$

where $|\psi_0\rangle = |01, 01\rangle$, $|\psi_1\rangle = |01, 10\rangle$, $|\psi_2\rangle = |10, 01\rangle$, $|\psi_3\rangle = |10, 10\rangle$, $|M^\pm\rangle = [|\psi_2\rangle \pm |\psi_1\rangle] / \sqrt{2}$, $s_i = a_i + b_i + 2(c_i + d_i)$, and the coefficients given as:

$$a_i = \frac{1}{2} \left[1 + \left(\frac{a - b}{a + b} \right)^{i-1} \left(\frac{a_e - b_e}{a_e + b_e} \right) \right] z_i, \quad (\text{S38})$$

$$b_i = \frac{1}{2} \left[1 - \left(\frac{a - b}{a + b} \right)^{i-1} \left(\frac{a_e - b_e}{a_e + b_e} \right) \right] z_i, \quad (\text{S39})$$

$$c_i = \frac{s_i}{4} \left[1 - \frac{z_i}{s_i(1 - 2w_r)} [(1 - 2w_r)(1 - 2w_1)]^{2^{i-1}} \right], \quad (\text{S40})$$

$$d_i = \frac{s_i}{4} - \frac{z_i}{2} \left[1 - \frac{1}{2(1 - 2w_r)} [(1 - 2w_r)(1 - 2w_1)]^{2^{i-1}} \right], \quad (\text{S41})$$

with $w_i = c_e/(a_e + b_e)$, $w_r = c/(a + b)$, $s_1 = a_e + b_e + 2c_e$, $s_i = s = a + b + 2c$, $2 \leq i \leq n + 1$, and z_i given by,

$$z_i = \left(\frac{s^2}{a + b} \right) \left(\frac{1}{(1 + 2w_1)(1 + 2w_r)} \right)^{2^{i-1}}, \quad i \geq 2, \quad (\text{S42})$$

with $z_1 = a_e + b_e$. The expressions for a_i , b_i , c_i , and d_i correctly reduce to a_e , b_e , c_e , and 0, respectively, for $i = 1$. As an example calculation, the fidelity of ρ_i (with respect to $|M^+\rangle$), $F_i = \sqrt{\langle M^+ | \rho_i | M^+ \rangle}$ is given by, $F_i = \sqrt{(a_i + d_i)/s_i}$.

Evaluating the formula for QBER

Proposition 11 Assume that Alice and Bob have made a measurement on ρ_i , $i \in \{1, \dots, n+1\}$. Conditioned on the fact that they get exactly one click each on their qubits (which happens with probability P_1 , as proven in Proposition 4), the probability Q_i , that they obtain a mismatched bit (a bit error) is given by,

$$Q_i = \frac{1}{2} \left[1 - \frac{t_d}{t_r} (t_r t_e)^{2^{i-1}} \right], \quad 1 \leq i \leq n+1, \quad (\text{S43})$$

where $t_e = (a_e + b_e - 2c_e)/(a_e + b_e + 2c_e)$, $t_r = (a + b - 2c)/(a + b + 2c)$, and $t_d = ((q_1 - q_2)/(q_1 + q_2))^2$ are loss-noise parameters of detectors in the elementary links, memory nodes, and Alice-Bob, respectively.

Proof. The first step is to show that Q_i can be expressed as follows:

$$Q_i = \frac{1}{2} [1 - t_d(1 - 2\zeta_i)], \quad (\text{S44})$$

where $\zeta_i = 2c_i/s_i$, $t_d = ((q_1 - q_2)/(q_1 + q_2))^2$. Since we have shown that $s_i = s = a + b + 2c$, $i \geq 2$, and $s_1 = a_e + b_e + 2c_e$, we only need to solve for c_i , in order to evaluate Q_i . In order to prove (S44), we can evaluate $Q_i = \text{Tr}[\rho_i(M_{0101} + M_{1010})]/\text{Tr}[\rho_i(M_{0101} + M_{0110} + M_{1001} + M_{1010})]$, where the denominator is P_1 . It is easy to argue (S44) informally as follows. We first note that ρ_i is of the form,

$$\rho_i = r_1|M^+\rangle\langle M^+| + r_2|M^-\rangle\langle M^-| + r_3|\psi_0\rangle\langle\psi_0| + r_4|\psi_1\rangle\langle\psi_1| + r_5|\psi_2\rangle\langle\psi_2| + r_6|\psi_3\rangle\langle\psi_3|, \quad (\text{S45})$$

with $\sum_{i=1}^6 r_i = 1$. $Q_i = (Q_1 + Q_2)/P_1$, where

$$Q_1 = q_1^2 r_3 + q_1 q_2 \left[r_4 + \frac{1}{2}(r_1 + r_2) + r_5 + \frac{1}{2}(r_1 + r_2) \right] + q_2^2 r_6, \quad \text{and} \quad (\text{S46})$$

$$Q_2 = q_2^2 r_3 + q_1 q_2 \left[r_4 + \frac{1}{2}(r_1 + r_2) + r_5 + \frac{1}{2}(r_1 + r_2) \right] + q_1^2 r_6, \quad (\text{S47})$$

since the relative contributions of $|\psi_0\rangle, |\psi_1\rangle, |\psi_2\rangle, |\psi_3\rangle$ in ρ_i are $r_3, r_4 + (r_1 + r_2)/2, r_5 + (r_1 + r_2)/2$, and r_6 respectively. Simplifying everything, and substituting $P_1 = (q_1 + q_2)^2$, we get,

$$Q_i = \left(\frac{q_1 - q_2}{q_1 + q_2} \right)^2 (r_3 + r_6) + \frac{2q_1 q_2}{(q_1 + q_2)^2}. \quad (\text{S48})$$

Now substituting $r_3 = r_6 = c_i/s_i$, defining $\zeta_i = 2c_i/s_i$, and $t_d = ((q_1 - q_2)/(q_1 + q_2))^2$, Eq. S44 follows.

We now divide $2c_i$ (from Eq. (S34)) by s_i to obtain,

$$\zeta_i = \frac{2c_i}{s_i} = \frac{1}{2} \left[1 - \frac{z_i}{\beta s_i} [\beta(1 - 2w_1)]^{2^{i-1}} \right]. \quad (\text{S49})$$

Substituting the expression for z_i above, and realizing that $s_i = s$, $i \geq 2$, and $s_1 = a_e + b_e + 2c_e$, it is easy to obtain the expression for Q_i in Eq. S43 after some algebraic manipulations. The $i = 1$ case must be handled separately (since $s_1 \neq s_i, i \geq 2$), but the final expression in Eq. S43 is valid for all $i = 1, 2, \dots, n+1$. ■

The following corollary is an interesting consequence of Eq. S43:

Corollary 12 The following law for error propagation holds through the successive connections of elementary links:

$$(1 - 2Q_{i+1}) = \frac{t_r}{t_d} (1 - 2Q_i)^2, \quad 1 \leq i \leq n. \quad (\text{S50})$$

An interesting thing to note about the error propagation is the constant $t_r = (1 - 2w_r)/(1 + 2w_r)$, which is a function of the parameter $2w_r = 2c/(a + b)$. We saw that when two pure bell states are ‘connected’ by a linear-optic BSM with lossy-noisy detectors, $2c$ is the fractional probability that spills over into classical correlations (the nonentangled part), and $a + b$ is the fractional probability that goes into one of two entangled bell states.

Putting everything together, we finally have an expression for the secret-key rate,

$$R = \frac{P_1 P_{\text{succ}} R_2(Q_{n+1})}{2T_q} \text{ secret-key bits/sec}, \quad (\text{S51})$$

where $P_{\text{succ}} = [4s(1 - (1 - 4s_1)^M)]^{2^n}/4s$, $P_1 = (q_1 + q_2)^2$, and $Q_{n+1} = \left[1 - \frac{t_d}{t_r} (t_r t_e)^{2^n} \right]/2$, are all defined in terms of the detector loss and noise parameters, and the total number of elementary links $N = 2^n$.

PROOF OF THE MODIFIED LOGISTIC MAP

In this section, we prove the following new variation of the logistic map, whose solutions are known to have chaotic behavior in general.

Theorem 13 *The quadratic difference equation, $w_{i+1} = w_r + 2(1 - 2w_r)w_i(1 - w_i)$, which is a variant of the logistic map $w_{i+1} = 2w_i(1 - w_i)$ with $R = 2$, can be exactly solved, and the solution is given by:*

$$w_i = \frac{1}{2} \left[1 - \frac{1}{\beta} [\beta(1 - 2w_1)]^{2^{i-1}} \right], i \geq 1, \quad (\text{S52})$$

where $\beta = 1 - 2w_r$, and the initial value w_1 specified.

Proof. We start with the solution to the standard logistic map with $R = 2$, i.e., with $w_r = 0$. The solution is given by:

$$w_i = \frac{1}{2} \left[1 - (1 - 2w_1)^{2^{i-1}} \right]. \quad (\text{S53})$$

We use the ansatz that the modified map has the solution of the form

$$w_i = \frac{1}{2} \left[1 - (1 - 2w_1)^{2^{i-1} + \xi_i} \right]. \quad (\text{S54})$$

Inserting this into the difference equation, we get

$$\frac{1}{2} \left[1 - (1 - 2w_1)^{2^{i+\xi_{i+1}}} \right] = w_r + \frac{(1 - 2w_r)}{2} \left[1 - (1 - 2w_1)^{2^{i+\xi_i}} \right]. \quad (\text{S55})$$

Letting $y_i = (1 - 2w_1)^{2^{i+\xi_i}}$ and $a = 1 - 2w_r$, we obtain

$$y_{i+1} = a^2 y_i^2, \quad (\text{S56})$$

which can be solved to obtain

$$y_i = \frac{1}{a^2} (a^2 y_1)^{2^{i-1}}, i \geq 1, \quad (\text{S57})$$

Using this to solve for ξ_i , we get

$$\xi_i = i - \log_2 \left[\frac{2^i \log_2(a(1 - 2w_1)) - \log_2(a^2)}{\log_2(1 - 2w_1)} \right]. \quad (\text{S58})$$

Finally, inserting the expression for ξ_i into the ansatz, we obtain the following expression for w_i .

$$w_i = \frac{1}{2} \left[1 - \frac{1}{a} (a(1 - 2w_1))^{2^{i-1}} \right], i \geq 1. \quad (\text{S59})$$

■

-
- [S1] A. Ekert, Phys. Rev. Lett. **67**, 6 (1991).
[S2] C. H. Bennett, G. Brassard, C. Crépeau, R. Jozsa, A. Peres, and W. K. Wootters, Phys. Rev. Lett. **70**, 1895–1899 (1993).
[S3] C. Bennett and S.J. Wiesner, Phys. Rev. Lett. **69**, 2881 (1992).
[S4] M. M. Wilde and M.-H. Hsieh, Quantum Information Processing **11**, 6, 1431–1463, (2012).
[S5] M. M. Wilde, P. Hayden, and S. Guha, Phys. Rev. Lett. **108**, 140501 (2012).
[S6] M. Takeoka, S. Guha, and M. M. Wilde, arXiv:1310.0129 [quant-ph] (2013).
[S7] N. Sangouard, C. Simon, H. de Riedmatten, and N. Gisin, Rev. Mod. Phys. **83**, 33 (2011).
[S8] H.-J. Briegel, W. Dür, J. I. Cirac, and P. Zoller, Phys. Rev. Lett. **81**, 5932 (1998).
[S9] L.-M. Duan, M. D. Lukin, J. I. Cirac, and P. Zoller, Nature **414**, 413–418, 22 November (2001).
[S10] L. Jiang, J. M. Taylor, K. Nemoto, W. J. Munro, R. V. Meter, and M. D. Lukin, Phys. Rev. A **79**, 032325, (2009).
[S11] S. Bratzik, H. Kampermann, and D. Bruß, Phys. Rev. A **89**, 032335 (2014).

- [S12] N. Sinclair, E. Saglamyurek, H. Mallazadeh, J.A. Slater, M. Hedges, M. George, R. Ricken, D. Oblak, W. Sohler, and W. Tittel, <http://arxiv.org/abs/1309.3202>.
- [S13] S. L. Braunstein, and A. Mann, Phys. Rev. A *Rapid Communications*, **51**, 3 (1995).
- [S14] N. Lütkenhaus, J. Calsamiglia, and K.-A. Suominen, Phys. Rev. A **59**, 3295 (1999).
- [S15] A. Khalique, W. Tittel, and B. C. Sanders, Phys. Rev. A **88**, 022336 (2013).
- [S16] M. Razavi, H. Farmanbar, and N. Lütkenhaus, Optical Fiber Communication (OFC) Conference, San Diego, California, United States, February 24-28, (2008).
- [S17] E. Schröder, “Über iterierte Funktionen”, Math. Ann. 3 (2): 296–322, doi:10.1007/BF01443992 (1870).
- [S18] E. Saglamyurek, N. Sinclair, J. Jin, J. A. Slater, D. Oblak, F. Bussi eres, M. George, R. Ricken, W. Sohler, W. Tittel, Nature **469**, 512 (2011).
- [S19] A. Ferenczi and N. L tkenhaus, Phys. Rev. A **85**, 052310 (2012).
- [S20] Zhao-Xi Xiong, Han-Duo Shi, Yi-Nan Wang, Li Jing, Jin Lei, Liang-Zhu Mu and Heng Fan, Phys. Rev. A, **85**, 012334 (2012).
- [S21] H. Krovi, Z. Dutton, S. Guha, C. A. Fuchs, W. Tittel, C. Simon, J. Slater, K. Heshami, M. Hedges, G. S. Kanter, Y.-P. Huang, C. Thiel, *to be published*, Proceedings of the Conference on Lasers and Electro-Optics (CLEO), June 8-13, San Jose, CA, (2014).
- [S22] W. P. Grice, Phys. Rev. A **84**, 042331 (2011).
- [S23] H. A. Zaidi and P. van Loock, Phys. Rev. Lett. **110**, 260501 (2013).